Screening of rare-earth-lean intermetallic 1-11 and 1-11-X compounds of YNi_9In_2-type for hard-magnetic applications

Wolfgang Körner,[1] Georg Krugel,[1] Daniel F. Urban,[1,*] and Christian Elsässer[1,2]

[1] *Fraunhofer Institute for Mechanics of Materials IWM, Wöhlerstr. 11, 79108 Freiburg, Germany*
[2] *University of Freiburg, Freiburg Materials Research Center, Stefan-Meier-Str. 21, 79104 Freiburg, Germany*

(Dated: December 13, 2018)

We report on theoretical investigations of ferromagnetic rare-earth-transition-metal phases with the structure of YNi_9In_2 and with additional atoms X at two interstitial positions. By a high-throughput-screening (HTS) approach based on density functional theory the intrinsic key properties of hard magnets, namely the magnetization M, energy product $(BH)_{max}$ and uniaxial magnetocrystalline anisotropy constant K_1 are estimated. The HTS identifies several promising phases $NdFe_{10}AX$ with A= Ti, V, Cr, Mn, Fe, Co, Ni, Cu, Zn, Al, Si, P, and X=B, C, N. These phases partially outperform $Nd_2Fe_{14}B$ in terms of $(BH)_{max}$ and K_1 values, and they contain about 35% less rare-earth atoms.

PACS numbers: 75.30.Gw, 75.40.Mg ,75.50.Ww

I. INTRODUCTION

The expanding market share of sustainable technologies like wind energy and electro-mobility will further increase the demand for high-performance hard magnets in the near future. Currently, $Nd_2Fe_{14}B$ doped with Dy is the benchmark and work-horse material in this field. But besides its moderate temperature performance it depends on the unforeseeable price development of the rare earth elements Nd and Dy. As a consequence, renewed world-wide research activities were started in recent years with the goal of finding new hard-magnetic compounds with comparable performance to $Nd_2Fe_{14}B$ but with significantly less or no contents of critical elements.[1,2]

One focus of recent experimental and theoretical studies[3–11] is on intermetallic phases with the $ThMn_{12}$ crystal structure. These phases are interesting due to their favorable composition ratio of rare-earth (RE) and transition metal (TM) elements, RE:TM=1:12, and their uniaxial, namely tetragonal, crystal structure which is a necessary condition for uniaxial magnetocrystalline anisotropy. A similar beneficial ratio RE:TM=1:13 can be obtained based on the $NaZn_{13}$-type crystal structure and its tetragonal $LaCo_9Si_4$ variant.[12,13,16]

In this paper, our theoretical screening approach is extended to the YNi_9In_2 structure type[14] having an attractive ratio of RE:TM=1:11. This structure is an ordered variant of $CeNi_5Mn_6$ in which the Ni and Mn atoms are randomly distributed over the TM sites.[15] Additionally, two variants of this 1-11 structure are considered. They are referred to as 1-11-X(2b) and 1-11-X(2d) in the following, and are obtained by inserting interstitial atoms on the unoccupied Wyckoff positions (2b) or (2d) of the YNi_9In_2 structure. It is shown that this kind of alloying with light interstitial elements X = B, C, or N can enhance the tetragonal distortion of the YNi_9In_2 structure. This geometric effect combined with chemical bonding effects of the interstitial X atoms[6–8,10,16] may increase the magnetocrystalline anisotropy significantly. Specifically, the results of our study indicate $NdFe_{11}X$ and $NdFe_{10}AX$ with substitutionals A = Ti, V, Cr, Mn, Co, Ni, Cu, Zn, Al, Si or P and interstitials X = B, C, or N at (2b) sites as RE-lean intermetallic RE-TM compounds with potentially good intrinsic hard-magnetic properties.

II. THEORETICAL APPROACH

A. Structure models

The tetragonal YNi_9In_2 crystal structure belongs to space group No. 127 (P4/mbm). The lattice parameters of $NdNi_9In_2$ and the internal parameters determined experimentally by Bigun et al.[30] were taken as starting point for the construction of the unit cell of the 1-11 structure which contains 24 atoms in total (see Fig. 1, left). Since the analysis is focused on hard-magnetic applications with high magnetization a substantial amount of Fe contents is required for promising compounds. Therefore, in order to have a realistic structure model for the screening, the $NdNi_9In_2$-type structure with Fe atoms set on all TM sites was structurally optimized using density functional theory (DFT) with VASP[32,33](see following section for computational details). The lattice and internal parameters of this $NdFe_{11}$ structure were taken as input for the HTS of the 1-11 compounds. Correspondingly, the two $NdFe_{11}N$ structure models, 1-11-X(2b) and 1-11-X(2d), each containing 26 atoms in the unit cell (see Fig. 1), were structurally optimized using VASP as well.

The structural parameters were kept fixed within the HTS procedure when substituting different RE, TM and interstitial elements (for discussion see our related work[10,16]). The structure parameters of $NdFe_{11}N$ were used as well for the HTS of phases containing B or C. Test calculations conducted a posteriori for the most promising candidate structures with optimized lattice and internal parameters of $NdFe_{11}B$ and $NdFe_{11}C$ indicated only

Typeset by REVTEX

small deviations (in the order of 1%) of the magnetic quantities relative to the results obtained with the structural parameters of $NdFe_{11}N$.

B. Structural relaxation with VASP

The structural optimization of the crystals was carried out using the projector augmented wave (PAW) method[31] as implemented in VASP.[32,33] The generalized gradient approximation (GGA)[34] was used for exchange-correlation, and PAW pseudopotentials with 14 and 5 valence electrons were used for Fe and N, respectively. For Nd we took the PAW potential which keeps the $4f$ electrons frozen in the core ("Nd_3").[35] The number of $4f$ electrons in the core equals the number of valence electrons minus 3 which is the formal valence.[35] Elastic stresses and interatomic forces were relaxed using the BFGS algorithm. The calculations were carried out with a plane-wave cutoff energy of 680 eV, $3\times3\times5$ Monkhorst-Pack[36] k-meshes and a Gaussian broadening of 0.05 eV.

C. Screening with TB-LMTO-ASA

The magnetic properties of the intermetallic compounds with the 1-11, 1-11-X(2b), and 1-11-X(2d) structures were examined using the HTS procedure set up by Drebov et al.[17] It allows a fully automated generation of new phases by combinatorial substitution of sets of equivalent atoms. Here, the Y-sites of the YNi_9In_2 structure were occupied either by Ce, Nd, or Sm. The TM sites, originally occupied with Ni or In, were decorated with a variety of magnetic transition metal elements, namely Cr, Mn, Fe, Co, and Ni, and non-magnetic elements Al, Si, P, Ti, V, Cu and Zn. For the 1-11-X compounds we additionally inserted X = B, C, or N as interstitial

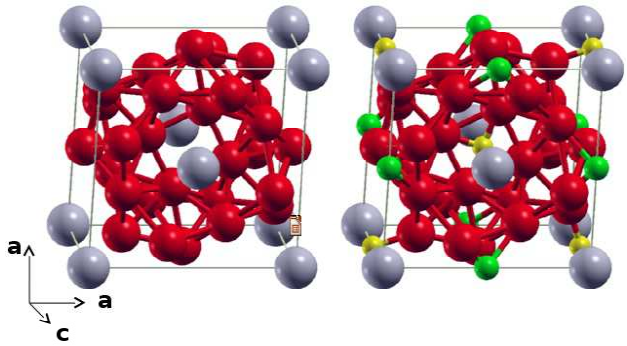

FIG. 1: (Color online) Structure models of $NdFe_{11}$ (left) and the two realizations of the corresponding 1-11-X phases (right). Large grey and red spheres represent Nd and Fe atoms, respectively. Small yellow spheres represent interstitial atoms X = B, C, or N on Wyckoff position 2b in $NdFe_{11}X$(2b). Alternatively, small green spheres represent interstitial atoms on Wyckoff position 2d in $NdFe_{11}X$(2d).

Lattice parameters	a [Å]	c [Å]	c/a	Volume [Å^3]
$NdFe_{11}$	8.206	4.808	0.586	323.76
$NdFe_{11}N$ (2b)	8.272	4.935	0.597	337.68
$NdFe_{11}N$ (2d)	8.313	4.894	0.589	338.12
$NdFe_{11}B$ (2b)	8.263	4.949	0.599	337.92
$NdFe_{11}C$ (2b)	8.230	4.990	0.606	337.92
$NdNi_9In_2$ [Ref. 30]	8.267	4.855	0.587	333.81

TABLE I: Lattice parameters of $NdFe_{11}$ and $NdFe_{11}X$ with interstitial element X at Wyckoff positions (2b) or (2d) which were obtained by DFT structural optimization. Experimental lattice parameters of $NdNi_9In_2$ taken from Bigun et al.[30] are given for comparison.

internal coordinate	x_{4g}	x_{8j}	y_{8j}	x_{8k}	z_{8k}
$NdFe_{11}$	0.615	0.067	0.216	0.178	0.238
$NdFe_{11}N$ (2b)	0.616	0.071	0.218	0.173	0.239
$NdFe_{11}N$ (2d)	0.652	0.078	0.209	0.165	0.240
$NdFe_{11}B$ (2b)	0.615	0.071	0.222	0.175	0.240
$NdFe_{11}C$ (2b)	0.615	0.070	0.217	0.174	0.240
$NdNi_9In_2$ [Ref. 30]	0.621	0.063	0.212	0.179	0.247

TABLE II: Internal structural parameters of $NdFe_{11}$ and $NdFe_{11}X$ as obtained by structural optimization with DFT. The rare-earth atoms are located at Wyckoff positions (2a), while the transition metal elements occupy the (2c), (4g), (8j) and (8k) Wyckoff positions. Interstitial atoms X are either located at Wyckoff positions (2b) or (2d). Representative coordinates for the individual Wyckoff groups are (0, 0, 0) for (2a), (0, 0, 0.5) for (2b), (0, 0.5, 0.5) for (2c), (0.5, 0.5, 0) for (2d), (x_{4g}, x_{4g}+0.5, 0) for (4g), (x_{8j}, y_{8j}, 0.5) for (8j), and (x_{8k}, x_{8k}+0.5, z_{8k}) for (8k). Experimental structural parameters of $NdNi_9In_2$ taken from Bigun et al.[30] are given for comparison.

elements. Overall, 1102 compounds containing Nd were assessed while for Ce and Sm we screened 453 compounds each.[42]

Total energies as well as spin polarized electronic states and densities from which the physical properties are derived are calculated with the tight-binding (TB) linear-muffin-tin-orbital (LMTO)[18] atomic-sphere approximation (ASA) method of DFT.[19,20] The TB-LMTO-ASA calculations were performed using the local spin-density approximation (LSDA), the scalar-relativistic approximation of Koelling and Harmon[21] and the exchange-correlation functional of von Barth and Hedin[22] in the parametrization of Moruzzi et al.[23] Since the LSDA

has a validity limited to weakly correlated systems, the strongly localized $4f$ electrons are treated by the "open core states" approach.[24,25] For the k-point sampling of the Brillouin-zone integrals the linear tetrahedron method and $6 \times 6 \times 10$ Monkhorst-Pack meshes were used. In the ASA the supercell volume is subdivided into spheres, and as in our previous work[10,17] we rely here on the well-tested ratio for the atomic-sphere radii $r(\mathrm{RE})/r(\mathrm{TM})/r(\mathrm{IS})$=1.35/1/0.7.[26]

The DFT calculations yield the essential intrinsic crystal properties for the intermetallic phases, namely the magnetization M, the local magnetic moments, the anisotropy constant K_1, and the relative phase stability energy ΔE_f. The anisotropy field can be estimated from K_1 and M via the heuristic formula $H_a = 2K_1/(\mu_0 M)$. The TB-LMTO-ASA method determines the single crystal magnetization in good accuracy which allows an estimation of the energy product $(\mathrm{BH})_{\max}$ via the heuristic formula $(\mathrm{BH})_{\max}^{EST} = (0.9\mu_0 M)^2/(4\mu_0)$. This implies the common assumption that ideally about 10% of a processed bulk hard-magnetic microstructure consists of non-magnetic phases.[6] The calculation of the magnetocrystalline anisotropy (in terms of first order anisotropy constants K_1) is based on the single ion anisotropy model. A brief summary of this approach and its restrictions can be found in our previous work.[16] For more details we refer the reader to the Refs. 10,20,27,28. The formation energy ΔE_f of an intermetallic phase is calculated with respect to its elemental constituents and is an approximate indicator on whether a phase may be stable.

For the magnetocrystalline anisotropy there is in general a systematic quantitative discrepancy between theoretical predictions and experimentally measured values which originates from the idealization in theory. Real materials contain point defects and extended defects and are thus structurally, chemically and magnetically inhomogeneous. In the theoretical model no such inhomogenities are included. It is assumed that the magnetization is rotated between the easy and hard directions of an uniaxially anisotropic magnetic single crystal by a homogeneous external magnetic field. For Ce the situation is even further complicated by its mixed valence. The theoretical model implies the fixed valence state 3+ whereas in reality the valence state of Ce depends on the compound. For a detailed discussion we refer the reader to Ref. 10 and references therein.

For the interpretation of the theoretical results as guidelines for experiments we have proposed heuristic adjustment factors:[10] in order to convert our zero-temperature single-domain DFT-HTS results for the magnetocrystalline anisotropy to room temperature estimates the theoretically obtained values for K_1 are divided by 4 for Nd and Sm. For Ce containing RE-TM-X compounds a division by 35 provides a conservative estimate. Hence theoretical predicted values of $K_1^{ASA} \geq 20$ MJ/m^3 for phases containing Nd and Sm, and of $K_1^{ASA} \geq 175$ MJ/m^3 for phases containing Ce, correspond to experimental target values of $K_1 \geq 5$ MJ/m^3 for very good hard magnets like $Nd_2Fe_{14}B$.

III. RESULTS AND DISCUSSION

A. Crystal structures

The lattice parameters obtained by our structural optimization are given in Table I. The 1-11-X(2b) and the 1-11-X(2d) structures have slightly larger unit cell volumes compared to the volume of the hypothetical $NdFe_{11}$. Their increase by the typical few percent is a result of the insertion of the light interstitial elements B, C, or N. The c/a ratios of the relaxed 1-11-X structures are only slightly larger than that of the relaxed 1-11 structure.

The calculated optimized internal parameters are given in Table II. Compared to the experimentally studied $NdNi_9In_2$,[30] replacing Ni and In by Fe atoms leads to very little internal rearrangement and a decrease of the lattice parameters a and c (and thus the volume). This effect is conceivable since the Fe atoms are of similar size compared to the Ni atoms but significantly smaller than the In atoms (metallic radii for 12-coordination are R_{Fe}=126 pm, R_{Ni}=125 pm, and R_{In}=167 pm, respectively).[29]

B. Results of the screening

The combinatorial screening of altogether over 2000 compounds[42] with 1-11 and 1-11-X structures revealed roughly 1100 magnetic compounds. A small selection of the HTS results for calculated magnetic properties is given in Table III. This selection was guided by the intention, on the one hand, to illustrate representative trends (e.g. how the magnetic properties change from Ce via Nd to Sm) and, on the other hand, to list the identified most promising hard-magnetic phases. Mainly structures with a large amount of Fe (at least 10 atoms per formula unit) appear in this list, as only these phases have sufficiently high magnetizations and energy products. The most promising phases are highlighted by bold font and further discussed below. Prior to that, the observed systematic trends are analyzed.

Note that all $NdFe_{10}AX$ compounds which are listed in Table III correspond to a substitution of element A on the Wyckoff site (2c). In a previous study we have shown for the case of $ThMn_{12}$-type compounds that the dependence of the magnetic quantities on the arrangement of substitutional TM atoms is not a critical issue for the HTS.[11]

1. Systematic trends

(1) Phase stability estimated from formation energies ΔE_f of the intermetallic compounds calculated relative

System	$(BH)_{max}^{EST}$ [kJ/m^3]	$\mu_0 M^{ASA}$ [T]	K_1^{ASA} [MJ/m^3]	ΔE_f [eV/atom]
$CeFe_{11}$	621	1.96	16	0.14
$CeFe_{10}Ti$	434	1.64	16	0.03
$CeFe_{11}N$	607	1.94	99	-0.34
$NdFe_{11}$	672	2.04	8	0.10
$NdFe_{10}Ti$	478	1.72	7	0.00
$NdFe_{11}N$	659	2.02	32	-0.39
$NdFe_{10}TiN$	513	1.78	32	-0.48
$NdFe_{10}VN$	503	1.77	31	-0.46
$NdFe_{10}CrN$	494	1.75	30	-0.42
$NdFe_{10}MnN$	493	1.75	30	-0.40
$NdFe_{10}CoN$	661	2.03	34	-0.39
$NdFe_{10}NiN$	639	1.99	34	-0.37
$NdFe_{10}CuN$	607	1.94	34	-0.34
$NdFe_{10}ZnN$	579	1.90	34	-0.39
$NdFe_{10}AlN$	543	1.83	34	-0.49
$NdFe_{10}SiN$	542	1.83	33	-0.57
$NdFe_{10}PN$	551	1.85	33	-0.60
$SmFe_{11}$	557	1.86	-15	0.07
$SmCo_{11}$	279	1.32	-23	0.09
$SmFe_{11}N$	551	1.85	-46	-0.42
$Nd_2Fe_{14}B$	556	1.87	19	-0.02
$Nd_2Fe_{14}B$ (exp.)	516[a]	1.86[b]	4.9[c]	
$Sm_2Fe_{17}N_3$	459	1.69	27	-0.82
$Sm_2Fe_{17}N_3$(exp.)	472[a]	1.54[c]	8.6[c]	
$SmCo_5$	174	1.04	69	0.06
$SmCo_5$ (exp.)	219[a]	1.07[c]	17.2[c]	

TABLE III: Selection of screening results. The magnetization M and the anisotropy constant K_1 calculated with TB-LMTO-ASA are listed along with the estimated energy product $(BH)_{max}^{EST} = (0.9M)^2/(4\mu_0)$. For comparison we added results for $Nd_2Fe_{14}B$, $Sm_2Fe_{17}N_3$ and $SmCo_5$ as benchmark materials with the highest energy product $(BH)_{max}$ and anisotropy constant K_1, calculated using the same theoretical approach. Experimental data taken from [a]Ref. 37 (Table 11.1 therein), [b]Ref. 38, and [c]Ref. 40 are given in brackets. The magnetization was determined experimentally at 4K whereas K_1 was measured at room temperature. The identified promising candidates for new hard-magnetic phases obtained from the HTS are highlighted by bold font. Note that the respective phases containing B or C instead of N have promising magnetic properties as well. All the interstitial 1-11-X structures listed here are of the (2b) type, and the substitutional alloying elements A are on the (2c) position.

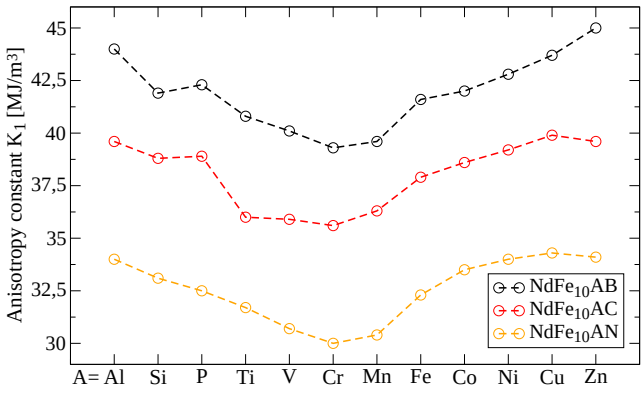

FIG. 2: (Color online) The calculated anisotropy constant K_1 for the different compounds $NdFe_{10}AX(2b)$ with X = B, C,

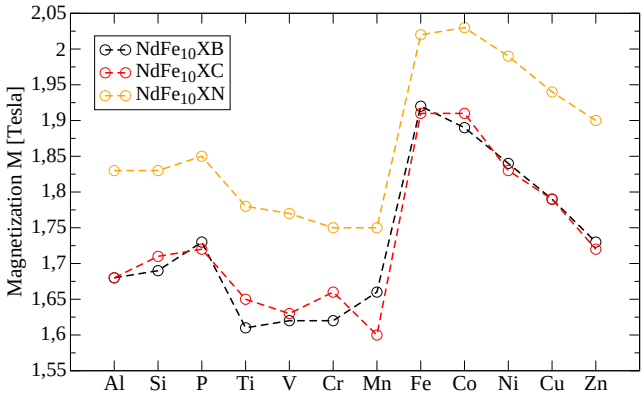

FIG. 3: (Color online) The calculated magnetization M for the different compounds $NdFe_{10}AX(2b)$ with X = B, C, or N.

to the elemental phases:

- In general, the 1-11-X structures have a more negative ΔE_f than the corresponding 1-11 structures (cf. Tab. III). The 1-11-X(2b) compounds have lower relative formation energies than the corresponding 1-11-X(2d) compounds, and these always have lower relative formation energies than the corresponding 1-11 phase. This stability hierarchy is important because the most stable 1-11-X(2b) compounds potentially have the highest K_1 values as well (see statement (2), below).

- The phase stability increases with the insertion of non-magnetic elements. Especially Ti, Al, Si, and P apparently stabilize the 1-11-X(2b) phases.

- Most 1-11-X compounds have negative formation energies relative to the elemental constituents. Nevertheless, the existence of more stable binary or ternary compounds cannot be excluded. Furthermore, since the TB-LMTO-ASA values for ΔE_f are only rough estimates, even calculated values which

are slightly positive may not yet exclude the existence of a phase (c.f. $SmCo_5$ in Table III).

(2) Magnetocrystalline anisotropy constants K_1:

- Comparing the three structure types, the 1-11-X(2b) compounds in general yield much larger K_1 values than the corresponding 1-11 and 1-11-X(2d) compounds which both have small K_1 values of about equal size. For example, K_1 of $CeFe_{11}$ is about a factor of five lower than K_1 of $CeFe_{11}X$ (X = B, C, or N) in the (2b) structure. For $NdFe_{11}$ and $NdFe_{11}N$(2d) the K_1 values are 8 MJ/m^3 and 5 MJ/m^3 compared to 32 MJ/m^3 of $NdFe_{11}N$(2b).
- The chemical influence of the interstitial atoms dominates the anisotropy constant K_1 since the differences in the internal and lattice parameters are rather small. We attribute the large deviations in the K_1 values from the 1-11-X(2b) to the 1-11-X(2d) compounds to their distinctly different interstitial sites. The Wyckoff sites (2b) are directly on the bond axes between two adjacent RE sites and therefore strongly influence the crystal field on the $4f$ states (distance $d_{RE-X} \approx 2.47$ Å). Placing the light interstitial atoms at the Wyckoff sites (2d) which are on the bond between two adjacent TM sites has a much weaker effect on the RE atoms (distance $d_{RE-X} \approx 4.16$ Å).
- All compounds containing Sm have negative or only slightly positive K_1 values. Thus they do not fulfill the requirement for strong uniaxial anisotropy which is indispensable for a good hard magnet. The opposite sign of K_1 for the phases containing Sm and Nd can be rationalized by the single-ion anisotropy model applied to the prolate and oblate shapes of the $4f$ electron densities of Sm and Nd, respectively, in the uniaxial crystal fields.[39,40]
- The anisotropy constant K_1 remains more or less constant when substituting one of the 11 Fe atoms by one of the considered elements.
- The dependence of K_1 on the interstitials B, C, or N for the 1-11-X(2b) phases is displayed in Fig. 2. For B one obtains a K_1 value which is 5-10% higher than for C and 10-20% higher than for N.

(3) Magnetization M:

- There is a clear trend for the 1-11-X(2b) phases that the magnetization M is highest for N as an interstitial atom. For C or B the values are lower and more or less equal (see Fig. 3). The same trend follows for the estimated energy product $(BH)^{EST}_{max}$ which is proportional to M^2.
- Substituting more than one Fe atom per formula unit in the 1-11, 1-11-X(2b) and 1-11-X(2d) structures by other elements leads to a dramatic decrease in the magnetization below 1.60 T which corresponds to an energy product $(BH)^{EST}_{max}$ below 400 kJ/m^3. The least decrease happens for the substitution of Fe by Co which is plausible.
- Some of the 1-11 compounds without interstitial atoms X reach high magnetizations and therefore potentially high energy products $(BH)^{EST}_{max}$ as can be seen from the upper part of Table III. But due to their low K_1 values the uniaxial orientation of the magnetization is not stable enough and these phases are not suitable hard magnet candidates.

2. *Promising hard-magnetic compounds*

The most promising candidates for new hard-magnetic phases obtained from the HTS, highlighted by bold font in Table III, fulfill the following criteria: energy product $(BH)^{EST}_{max} \geq 400$ kJ/m^3 and $K_1 \geq 20$ MJ/m^3 for Nd and Sm.

Very high magnetization values are obtained for $NdFe_{11}X$ with X=B, C, or N. Converting the calculated 32 Tesla ($T = 0$ K) for $NdFe_{11}N$ by the division of 4 (conversion factor for Nd, see section II C) leads to the experimentally expectable estimate of about 8 Tesla at room temperature. An even higher estimated value of about 10.5 Tesla is obtained for $NdFe_{11}B$ but at the price of a lower magnetization value.

A partial substitution of Fe by Co also leads to promising compounds like $NdFe_{10}CoX$ with X=B, C, or N. $NdFe_{10}CoN$ gives the highest magnetization and the largest estimated energy product $(BH)^{EST}_{max}$ of all considered compounds. The latter corresponds to an increase of 19% with respect to $Nd_2Fe_{14}B$.

The increase of the Co content is also expected to increase the Curie temperature as observed for many intermetallic phases.[1,41] For example, Buschow et al. found for the 1-11 phase $Gd(Fe_{1-x}Co_x)_9Ti_2$ (without interstitial atoms) that up to 50% Co content is needed in order to obtain T_C values of 500K.[41]

The insertion of non-magnetic alloying elements Cu, Zn, Ti, V, Si, Al, or P in small amounts leads to a decrease of the magnetization which is accompanied in most cases by a slight increase of the anisotropy constant K_1. Their higher relative phase stability makes them promising compounds for hard-magnetic applications.

C. Validation of HTS approach

The list of best candidates predicted by our HTS can a posteriori be used to validate the approach of using fixed input geometries (cf. Tabs. I and II) for the screening of the topologically closed packed 1-11 structure type. We have therefore optimized each structure using VASP with the computational setup described in Sec. II B. The results are summarized in Tab. IV where the first three columns list the changes of the total energy, volume and c/a ratio as result of the full relaxation of interatomic

System	$\Delta E_{\rm tot}$ [eV]	ΔV [Å^3]	$\Delta(\frac{c}{a})$	$\mu_0\Delta M^{\rm ASA}$ [T]	$\Delta K_1^{\rm ASA}$ [MJ/m^3]
$NdFe_{10}TiN$	-0.35	+9.4	-0.010	-0.01	+3
$NdFe_{10}VN$	-0.07	+3.6	-0.005	+0.01	+3
$NdFe_{10}CrN$	-0.04	+0.4	-0.005	± 0.	+5
$NdFe_{10}MnN$	0.	-1.6	-0.007	+0.04	+9
$NdFe_{10}CoN$	-0.01	+0.2	-0.002	± 0.	+2
$NdFe_{10}NiN$	-0.04	+0.5	-0.005	± 0.	+5
$NdFe_{10}CuN$	-0.14	+3.2	-0.007	-0.01	+5
$NdFe_{10}ZnN$	-0.28	+7.2	-0.006	+0.01	+2
$NdFe_{10}AlN$	-0.22	+5.7	-0.010	-0.01	+6
$NdFe_{10}SiN$	-0.05	-3.3	-0.004	± 0.	+5
$NdFe_{10}PN$	-0.15	-7.6	+0.006	± 0.	-2

TABLE IV: Change in total energy per unit cell, volume and c/a-ratio as obtained by VASP structural optimization with respect to the initial geometry used for the screening with V_0 =338.3Å^3 and $(c/a)_0$ = 0.598. The respective changes in magnetization $\mu_0\Delta M$ and anisotropy constant ΔK_1 were subsequently calculated with TB-LMTO-ASA.

forces and stresses. In a final step we have calculated the magnetization and anisotropy using TB-LMTO-ASA for these fully relaxed structures. The changes with respect to the values obtained with the fixed input geometry used for the screening are given in the last two columns of Tab. IV. The adjustments of energy, volume and aspect ratio are small for all structures considered and the magnetization essentially does not change (at the given level of precision). The anisotropy constant K_1 increases for all structures except the one containing phosphor. This can be essentially attributed to the adjustment of the c/a ratio. Altogether, these results corroborate the validity of our screening approach.

IV. SUMMARY

By means of electronic-structure calculations using the fast and efficient TB-LMTO-ASA method we have screened the magnetic properties of over 2000 different RE-TM-X compounds with 1-11 and 1-11-X structures as potential candidates for new hard-magnetic phases. Two 1-11-X(2b) and 1-11-X(2d) structures were derived from the 1-11 structure of YNi_9In_2 by decoration with interstitial elements on (2b) or (2d) sites.

Several systematic trends were identified. Most importantly some phases with 1-11-X(2b) structure combine high magnetization M, the highest anisotropy constants K_1 and the highest energetic stability.

The HTS has led to several promising phases based on $NdFe_{11}X$ with X = B, C, or N. Namely, $NdFe_{10}AX$ with A= Ti, V, Cr, Co, Ni, Cu, Zn, Al, Si, or P yield estimated energy products $(BH)_{\rm max}$ higher than 400 kJ/m^3 combined with K_1 values that are potentially larger than that of $Nd_2Fe_{14}B$. Thus they fulfill the targeted requirements for permanent magnet applications. Experimental efforts are encouraged to synthesize such hard-magnetic phases and to optimize their microstructure in order to obtain good permanent magnets.

V. ACKNOWLEDGMENTS

Financial support for this work was provided by the Fraunhofer Lighthouse Project *Critical Rare Earths*.

* Electronic address: daniel.urban@iwm.fraunhofer.de

[1] J. M. D. Coey, IEEE. Trans. Mag. **47**, 4671 (2011).
[2] O. Gutfleisch, M. A. Willard, E. Brück, C. H. Chen, S. G. Sankar and J. P. Liu, Adv. Mat. **23** (7), 821 (2011).
[3] C. Zhou, F. E. Pinkerton and J. F. Herbst, J. Appl. Phys. **115**, 17C716 (2014).
[4] C. Zhou, F. E. Pinkerton and J. F. Herbst, Scripta Mat. **95**, 66 (2015).
[5] D. Goll, R. Löffler, R. Stein, U. Pflanz, S. Goeb, R. Karimi, G. Schneider, Phys. Stat. Sol. RRL **8**, 865 (2014).
[6] Y. Hirayama, Y. K. Takahashi, S. Hirosawa, and K. Hono, Scripta Mat. **95**, 70 (2015).
[7] T. Miyake, K. Terakura, Y. Harashima, H. Kino and S. Ishibashi, J. Phys. Soc. of Japan **83**, 043702 (2014).
[8] Y. Harashima, K. Terakura, H. Kino, S. Ishibashi and T. Miyake, JPS Conf. Proc. **5**, 011021 (2015).
[9] Y. Harashima, K. Terakura, H. Kino, S. Ishibashi and T. Miyake, Phys. Rev. B 92, 184426 (2015).
[10] W. Körner, G. Krugel and C. Elsässer, Sci. Rep. **6**, 24686 (2016).
[11] T. Butcher, W. Körner, G. Krugel and C. Elsässer, J. Magn. Magn. Mat. **441**, 1-5 (2017).
[12] M. Pani, P. Manfrinetti, A. Provino, Fang Yuan, Y. Mozharivskyj, A.V. Morozkin, A.V. Knotko, A.V. Garshev, V.O. Yapaskurt and O. Isnard, J. Solid State Chem. **210**, 45, (2014).
[13] H. Michor, M. El-Hagary, M. Della Mea, M. W. Pieper, M. Reissner, G. Hilscher, S. Khmelevskyi, P. Mohn, G. Schneider, G. Giester and P. Rogl, Phys. Rev. B **69**, 081404 (2004).
[14] Ya. M. Kalychak, L. G. Akselrud, V. I. Zaremba and V. M. Baranyak, Dop. Akad. Nauk Ukr. RSR, Ser. B **8**, 35 (1984).
[15] Ya. M. Kalychak, L. G. Akselrud, Y. P. Yarmolyuk, O. I. Bodak, E. I. Gladyshevsky, Kristallografia **20**, 1045 (1984).
[16] G. Krugel, W. Körner, O. Gutfleisch and C. Elsässer, submitted (2016).
[17] N. Drebov, A. Martinez-Limia, L. Kunz, A. Gola, T. Shige-

matsu, T. Eckl, P. Gumbsch and C. Elsässer, New J. of Phys. **15**, 125023 (2013).
[18] O. K. Andersen: Phys. Rev. B **12**, 3060 (1975).
[19] K. Hummler and M. Fähnle, Phys. Rev. B **45**, 3161 (1992).
[20] M. Fähnle, K. Hummler, M. Liebs, T. Beuerle, Appl. Phys. A **57**, 67 (1993).
[21] D. D. Koelling and B.N. Harmon, J. Phys. C: Solid State Phys. **10**, 3107 (1977).
[22] U. von Barth and L. Hedin, J. Phys. C: Solid State Phys. **5**, 1629 (1972).
[23] V. L. Moruzzi, J.F. Janak, A.R. Williams: *Calculated Electronic Properties of Metals*, Pergamon, New York (1978).
[24] M. S. S. Brooks, L. Nordström and B. Johannson, J. Phys. Cond. Mat. **2**, 2357 (1991).
[25] M. S. S. Brooks, L. Nordström and B. Johannson, J. Phys. Cond. Mat. **3**, 3393 (1991).
[26] T. Beuerle and M. Fähnle, Phys. Stat. Solidi B **174**, 257 (1992).
[27] M. Richter, P. M. Oppeneer, H. Eschrig and B. Johansson, Phys. Rev. B **46**, 13919 (1992).
[28] M. Richter, J. Phys. D, Appl. Phys. **31**, 1017 (1998).
[29] A.F. Wells, "Structural Inorganic Chemistry," 5th ed., Clarendon Press, Oxford, 1984, p. 1288.
[30] I. Bigun, M. Dzevenko, L. Havela and Ya. Kalychak, Eur. J. Inorg. Chem. **16**, 2631 (2014).
[31] P. E. Blöchl, Phys. Rev. B **50**, 17953 (1994).
[32] G. Kresse and J. Furthmüller, Phys. Rev. B **54**, 11169 (1996).
[33] G. Kresse and D. Joubert, Phys. Rev. B **59**, 1758 (1999).
[34] J. P. Perdew, K. Burke, and M. Ernzerhof, Phys. Rev. Lett. **77**, 3865 (1996).
[35] For details on PAW potentials provided with VASP see http://cms.mpi.univie.ac.at/vasp/vasp/PAW_potentials.html
[36] H. J. Monkhorst and J.D. Pack, Phys. Rev. B **13**, 5188 (1976).
[37] K. H. J Buschow: *Concise Encyclopedia of Magnetic and Superconducting Materials*, Elsevier (2005), Second Ed., chapter Rare Earth Magnets: Materials (Table I).
[38] J. F. Herbst, Rev. Mod. Phys. **63**, 819 (1991).
[39] J. M. D. Coey, Phys. Scripta. **T39**, 21-28 (1991).
[40] J. M. D. Coey: *Magnetism and magnetic materials*, Cambridge University Press (2010).
[41] K. H. J. Buschow, D. B. de Mooij, M. Brouhs, H. H. A. Smit and R. C. Thiel, IEEE. Trans. Mag. **24**, 1611 (1988).
[42] For each structure, $ReFe_{11-n}A_n$ or $ReFe_{11-n}A_nX$, of given RE, A and X elements, there are 15 possibilities to populate the four types of Wyckoff positions by element A instead of Fe. Additionally, there is always the pure $ReFe_{11}$ or $ReFe_{11}X$ phase. For Nd we have screened the whole set of interstitials, X=B, C, and N, while for Sm and Ce we have restricted the analysis to X=N. Substitution by A=Al was only considered for the most promising $NdFe_{11-n}A_n$:N (2b) structure type.